Decorated Pt Nanoparticles

DOI: 10.1002/anie.201002501

Pd Adatom Decorated (100) Preferentially Oriented Pt Nanoparticles for Formic Acid Electrooxidation**

*Francisco J. Vidal-Iglesias, José Solla-Gullón, Enrique Herrero, Antonio Aldaz, and Juan M. Feliu**

Electrooxidation of formic acid on Pt has been extensively studied, mainly for its role in fuel cell applications and as a model for understanding fundamental aspects of electrocatalytic reactions. Complete oxidation of formic acid to CO_2 is a seemingly simple, two-electron process; however, intermediates of the reaction are adsorbed on and often poison the Pt surface.[1] In fact, the reaction mechanism follows two parallel paths, namely, direct oxidation to CO_2 and poisoning, which involves a dehydration step to yield water and adsorbed CO and its further oxidation to CO_2 at high potentials.[1] Modification of Pt by surface adatoms is known to enhance the rate of conversion of formic acid to CO_2, at least in part by altering the catalyst selectivity toward different pathways. Amid the adatoms investigated, Pd has been shown to greatly improve the kinetics of formic acid oxidation over Pt. The highest gains have been observed for Pt(100) electrodes decorated by Pd adatoms, for which decreased surface poisoning and lowering of the onset potential for formic acid oxidation to values as low as 0.12 V result.[2] In addition to bulk Pt single-crystal surfaces, adatom modification strategies also have been applied to nanometer-sized Pt electrocatalysts (e.g., Ru,[3–5] Au,[6] Pd,[7] Tl,[8] Pb,[8] and Bi[5,8,9]). Nevertheless, in most of these cases, the surface structure of the Pt nanoparticles was not specifically controlled, and consequently the results can not be properly compared with those obtained with model single-crystal electrodes.

In recent years, the shape of Pt nanoparticles, and therefore the crystallographic orientation of the atoms at their surface, has been reported to be of central importance.[10] Thus, some electrochemical reactions, including formic acid oxidation, have been studied to evaluate this effect.[11] Nevertheless, the use of adatoms to selectively decorate the surface of these shape-controlled Pt nanoparticles and consequently enhance their electrochemical properties, as previously reported in studies on Pt single crystals, has been scarcely evaluated. In addition to this enhanced activity, this new approach also would allow relationships between studies on bulk single crystals and nanoparticle catalysis to be properly established.

Somorjai et al. recently reported electrooxidation of formic acid using cubic Pt nanoparticles as seeds on which Pd was chemically deposited to form core/shell Pt/Pd nanocubes.[12] Nevertheless, this approach is appreciably different to those used for Pt(100) single-crystal electrodes, and the massive deposition of palladium does not allow information to be gained in the submonolayer adatom range in which maximum activities are reached on Pt(100) substrates.[2]

Herein we report for the first time the preparation of Pd adatom modified (100) preferentially oriented (cubic) Pt nanoparticles and their enhanced activity in electrooxidation of formic acid. Pd adatom deposition is electrochemically followed by cycling the electrode potential between two suitable limits in a solution containing a low Pd^{2+} concentration (10^{-5} M), in a similar way to that described in single-crystal studies.[2a,13] Thus, the voltammetric changes in each cycle, due to increasing amounts of Pd on the platinum surfaces can be monitored in situ. Therefore, the studies previously performed on Pt single crystals[2] can be exactly reproduced on the cubic Pt nanoparticles, and consequently relationships between single-crystal and nanoparticle catalysis can be properly established. Additionally, for the sake of comparison, the same Pd adatom decoration has been performed on quasispherical (nonpreferentially oriented) Pt nanoparticles, where electrocatalysis will also take place, although to a minor extent.

The cubic Pt nanoparticles were obtained by a colloidal method using sodium polyacrylate as capping material.[14] This surface-stabilizing agent weakly interacts with the platinum surface and therefore is easy to remove, which is crucial when the surface properties of the nanoparticles are under investigation. On the other hand, the nonpreferentially oriented Pt nanoparticles were synthesized in a water-in-oil microemulsion and further cleaned as previously described.[15]

Figure 1 shows TEM images of the two different types of Pt nanoparticles. Figure 1 A shows low- and high-resolution TEM images of the cubic Pt nanoparticles prepared by the colloidal method (additional TEM images are included in the Supporting Information, Figure S1). A preferential cubic shape is observed which suggests the existence of a significant amount of (100) sites at their surface. The average particle size is 8.2 ± 1.6 nm (see particle size histogram in Supporting Information, Figure S2). Figure 1 B shows a TEM image of nanoparticles prepared in microemulsion. These particles have a quasispherical shape and average size of 4.0 ± 0.6 nm

[*] Dr. F. J. Vidal-Iglesias, Dr. J. Solla-Gullón, Prof. E. Herrero, Prof. A. Aldaz, Prof. J. M. Feliu
Institute of Electrochemistry, University of Alicante
Apartado 99, 03080 Alicante (Spain)
Fax: (+34) 96-590-3537
E-mail: juan.feliu@ua.es
Homepage: http://web.ua.es/en/eqsup

[**] This work has been financially supported by the MICINN (Feder) of Spain and Generalitat Valencia through projects CTQ2006-0471/BQU and PROMETEO/2009/45. F.J.V.I. also thanks the European Social Funding.

Supporting information for this article is available on the WWW under http://dx.doi.org/10.1002/anie.201002501.

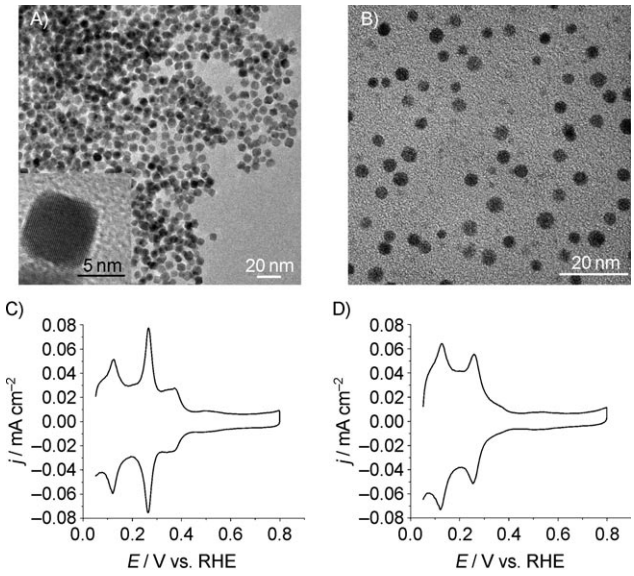

Figure 1. TEM images of cubic (A) and quasispherical (B) platinum nanoparticles and their corresponding voltammetric profiles in 0.5 M H_2SO_4 at 50 mV s^{-1} (C and D, respectively).

(see particle size histogram in Supporting Information, Figure S2) and can be considered as representative of polyoriented, nonspecifically structured, polycrystalline material. Figure 1C and D show the voltammetric profiles of the Pt nanoparticles in sulfuric acid solution. The definition and the symmetry of the adsorption states is evidence of the surface cleanliness, an indispensable prerequisite for correct in situ surface characterization. The presence of (100) sites is denoted by the peaks at 0.27 V and 0.37 V, characteristic of (100) edge (and corner) sites and (100) wide terraces, respectively.[16] Thus, comparison of the voltammetric fingerprints in 0.5 M H_2SO_4 clearly shows that cubic nanoparticles (Figure 1C) contain a higher proportion of (100) sites, especially in the two-dimensional domains, than the quasispherical nanoparticles (Figure 1D).

Figure 2 shows the evolution of the voltammograms during Pd incorporation on the surface for both Pt nanoparticle samples. In each case, the peaks corresponding to Pt

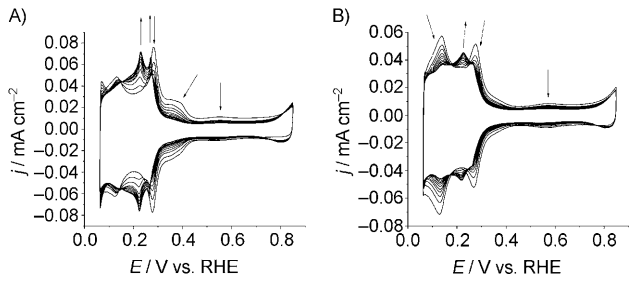

Figure 2. Evolution of the voltammetric profiles of the cubic (A) and quasispherical (B) platinum nanoparticles with increasing amounts of Pd on the surface. The first cycle and one every 20 cycles up to 200 cycles are shown. Test solution: 0.1 M $H_2SO_4 + 10^{-5}$ M $PdSO_4$. Sweep rate: 50 mV s^{-1}. Arrows indicate evolution of the peaks with increasing amount of deposited Pd.

diminish progressively in successive cycles. At the same time, a new contribution starts to appear between 0.15 and 0.27 V with a main peak centered at 0.23 V. This contribution can be ascribed to Pd deposited in the first layer on Pt(100) and Pt(111) surface terrace sites[13] (Figures S3 and S4 in Supporting Information). For the quasispherical Pt nanoparticles (Figure 2B) a similar evolution is observed, although to a lesser extent, due to the lower fraction of (100) and (111) terraces on the surface of the nanoparticles (see Supporting Information, Table S1). Interestingly, the Pt-related peaks are not fully replaced, that is, the Pd coverages lie below monolayer completion. The Pd coverage was estimated by measuring the decrease of the charge related to the (100) and (111) Pt terraces as a function of the number of Pd deposition cycles. The results are shown in Table 1, and additional data

Table 1: Current densities [μA cm^{-2}] after 10 min for oxidation of formic acid in chronoamperometric experiments. Test solution: 0.5 M H_2SO_4 + 0.1 M HCOOH, step potential: 0.2 V vs RHE.

	$Pt_{spherical}$	θ_{Pd}[a]	Pt_{cubic}	θ_{Pd}[a]
Bare Pt	0.0	0	0.5	0
50 cycles Pd	2.2	0.16	8.3	0.26
100 cycles Pd	4.6	0.37	19.4	0.45
150 cycles Pd	11.0	0.39	36.5	0.58
200 cycles Pd	18.0	0.58	65.5	0.63

[a] Fractional Pd coverage.

can be found in the Supporting Information (Figures S5 and S6). The Pd coverages are similar for both Pt nanoparticle samples and lie in the submonolayer range, in which maximum activities for formic acid electrooxidation were reported in previous studies on Pt single crystals[2].

Figure 3 shows responses for oxidation of formic acid on cubic and quasispherical platinum nanoparticles containing different amounts of deposited palladium (from zero to 200 cycles, every 50 cycles). For the bare cubic Pt nanoparticles, the oxidation current is strongly inhibited through the positive scan, since the (100) surface sites are almost

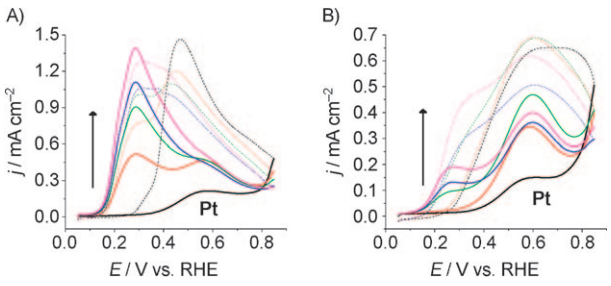

Figure 3. Voltammetric profiles for electrooxidation of formic acid with bare (black line) cubic (A) and quasispherical (B) Pt nanoparticles and with increasing amounts of Pd on the surface (after 50 (red line), 100 (green line), 150 (blue line) and 200 (magenta line) cycles under following conditions). Test solution: 0.5 M H_2SO_4 + 0.1 M HCOOH, sweep rate: 20 mV s^{-1}. Third cycles are shown. Solid and dashed lines represent the positive- and negative-going potential sweeps, respectively. Arrows indicate the evolution of the peaks with an increasing amount of deposited Pd.

completely poisoned by CO. At potentials above 0.8 V, the CO adlayer is oxidatively stripped, giving rise to a clean Pt surface. In the negative scan, the oxidation current increases as the potential is made more negative, until maximum current is obtained at about 0.48 V. From this point, adsorbed CO from dissociative adsorption of formic acid blocks the surface for the direct oxidation pathway, and the oxidation current diminishes until negligible values are obtained at about 0.3 V.[17] This strong hysteresis is close to that characteristic of a single-crystal Pt(100) surface, which is very active for both the direct oxidation pathway and surface poisoning.[16]

When Pd is incorporated on the surface, a new contribution at about 0.25 V is observed in the positive scan, which grows as the palladium coverage increases. Simultaneously, in the negative scan, the oxidation signal associated with free Pt sites diminishes. Consequently, the presence of Pd hinders CO formation in the low-potential range and shifts the oxidation onset potential to a much lower value (0.1 V), even when compared to that measured for Pt(100) in the absence of poisoning.[17] The evolution of the voltammetric profile with increasing amounts of Pd can be compared with that previously reported for a Pd-modified Pt(100) single crystal.[2]

To more thoroughly evaluate the effect of the surface structure, electrooxidation of formic acid also was performed on Pd-modified quasispherical Pt nanoparticles (Figure 3B). For the bare nanoparticles, the voltammetric profile is similar to that described for a polyoriented surface.[18] In the positive-going sweep, currents are again very low due to CO poisoning. The activity in the negative-going sweep is higher, but significantly lower than that obtained in the preceding case, because of the fewer (100) sites present, and thus confirms the structure sensitivity of formic acid electrooxidation on Pt.[11d,13] During Pd incorporation, the modifications are similar to those observed on cubic Pt nanoparticles. Pd on Pt always enhances formic acid oxidation, but, due to the lower fraction of (100) Pt sites in the quasispherical Pt nanoparticles, the relative intensity of the oxidation process in the low-potential region is much lower than in case of the cubic Pt nanoparticles.

To check more realistic conditions, chronoamperometric experiments were carried out at a potential as low as 0.2 V for 10 min. The results are reported in the Supporting Information, Figure S7, and Table 1 summarizes the final current densities as a function of the number of cycles of Pd deposition. While the obtained current densities for the bare Pt nanoparticles are almost negligible, those obtained after Pd decoration significantly increase with surface modification. Notably, the current densities obtained for the cubic Pt nanoparticles are considerably higher than those obtained for quasispherical Pt nanoparticles, that is, control of the surface structure/shape of the Pt nanoparticle substrates is of outstanding importance to optimize electrocatalyst activity.

In summary, the present results demonstrate that the use of adatom-decorated shape-controlled Pt nanoparticles is an interesting strategy to enhance electrocatalytic activity. These findings open the possibility of designing new and better electrocatalytic materials by means of the knowledge acquired in previous single-crystal studies.

Experimental Section

Experimental details of the synthesis and cleaning of the Pt nanoparticles are included in the Supporting Information. The electrochemical measurements were performed in 0.5 M H_2SO_4 solution at room temperature. Electrolyte solutions were prepared from Milli-Q water and Merck p.a. sulfuric acid on every day an experiment was carried out. A three-electrode electrochemical cell was used. The electrode potential was controlled by an Autolab PGSTAT30 system. The counterelectrode was a gold wire. Potentials were measured against a reversible hydrogen electrode (RHE) connected to the cell through a Luggin capillary. Before each experiment, the glassy carbon collector was mechanically polished with alumina and rinsed with ultrapure water to eliminate the nanoparticles from previous experiments. The active surface area of the Pt nanoparticles was determined by the charge involved in the so-called hydrogen UPD region (between 0.05 and 0.4 V) assuming 0.21 $mC\,cm^{-2}$ for the total charge after subtraction of the double-layer charging contribution.[19] The methodology employed for the Pd adlayer was similar to that previously reported for Pt single crystals.[20] The experimental details are included in the Supporting Information.

Received: April 27, 2010
Published online: August 16, 2010

Keywords: decoration · electrochemistry · nanocubes · palladium · platinum

[1] a) N. M. Markovic, P. N. Ross, *Surf. Sci. Rep.* **2002**, *45*, 117–229; b) E. Herrero, J. Feliu in *Encyclopedia Electrochemistry, Vol. 2* (Eds: A. J. Bard, M. Stratmann, E. J. Calvo), VCH, Weinheim, **2003**, pp. 443–465; c) J. M. Feliu, E. Herrero in *Handbook of Fuel Cells* (Eds.: W. Vielstich, A. Lamm, H. Gasteiger), Wiley, Chichester, UK, **2003**, p. 625, and references therein.

[2] a) M. J. Llorca, J. M. Feliu, A. Aldaz, J. Clavilier, *J. Electroanal. Chem.* **1994**, *376*, 151–160; b) M. Baldauf, D. M. Kolb, *J. Phys. Chem.* **1996**, *100*, 11375–11381; c) M. Arenz, V. Stamenkovic, T. J. Schmidt, K. Wandelt, P. N. Ross, N. M. Markovic, *Phys. Chem. Chem. Phys.* **2003**, *5*, 4242–4251.

[3] Y. Y. Tong, H. S. Kim, P. K. Babu, P. Waszczuk, A. Wieckowski, E. Oldfield, *J. Am. Chem. Soc.* **2002**, *124*, 468–473.

[4] P. Waszczuk, J. Solla-Gullón, H. S. Kim, Y. Y. Tong, V. Montiel, A. Aldaz, A. Wieckowski, *J. Catal.* **2001**, *203*, 1–6.

[5] Y. Du, C. Wang, *Mater. Chem. Phys.* **2009**, *113*, 927–932.

[6] P. Del Angel, J. M. Dominguez, G. D. Angel, J. A. Montoya, E. L. Pitara, S. Labruquere, J. Barbier, *Langmuir* **2000**, *16*, 7210–7217.

[7] P. Waszczuk, T. M. Barnard, C. Rice, R. I. Masel, A. Wieckowski, *Electrochem. Commun.* **2002**, *4*, 599–603.

[8] A. Kelaidopoulou, E. Abelidou, G. J. Kokkinidis, *J. Appl. Electrochem.* **1999**, *29*, 1255–1261.

[9] S. Daniele, S. Bergamin, *Electrochem. Commun.* **2007**, *9*, 1388–1393.

[10] a) Y. Xia, Y. Xiong, B. Lim, S. E. Skrabalak, *Angew. Chem.* **2009**, *121*, 62–108; *Angew. Chem. Int. Ed.* **2009**, *48*, 60–103; b) J. Chen, B. Lim, E. P. Lee, Y. Xia, *Nano Today* **2009**, *4*, 81–95; c) H. Lee, S. E. Habas, S. Kweskin, D. Butcher, G. A. Somorjai, P. Yang, *Angew. Chem.* **2006**, *118*, 7988–7992; *Angew. Chem. Int. Ed.* **2006**, *45*, 7824–7828.

[11] a) N. Tian, Z.-Y. Zhou, S.-G. Sun, Y. Ding, L. W. Zhong, *Science* **2007**, *316*, 732–735; b) C. Wang, H. Daimon, Y. Lee, J. Kim, S. Sun, *J. Am. Chem. Soc.* **2007**, *129*, 6974–6975; c) C. Wang, H. Daimon, T. Onodera, T. Koda, S. Sun, *Angew. Chem.* **2008**, *120*, 3644–3647; *Angew. Chem. Int. Ed.* **2008**, *47*, 3588–3591; d) J. Solla-Gullón, F. J. Vidal-Iglesias, A. López-Cudero, E. Garnier,

J. M. Feliu, A. Aldaz, *Phys. Chem. Chem. Phys.* **2008**, *10*, 3689 – 3698.
[12] H. Lee, S. E. Habas, G. A. Somorjai, P. Yang, *J. Am. Chem. Soc.* **2008**, *130*, 5406 – 5407.
[13] M. J. Llorca, J. M. Feliu, A. Aldaz, J. Clavilier, *J. Electroanal. Chem.* **1993**, *351*, 299 – 319.
[14] a) T. S. Ahmadi, Z. L. Wang, T. C. Green, A. Henglein, M. A. El-Sayed, *Science* **1996**, *272*, 1924 – 1926; b) J. Solla-Gullón, P. Rodríguez, E. Herrero, A. Aldaz, J. M. Feliu, *Phys. Chem. Chem. Phys.* **2008**, *10*, 1359 – 1373.
[15] a) J. Solla-Gullón, V. Montiel, A. Aldaz, J. Clavilier, *J. Electroanal. Chem.* **2000**, *491*, 69 – 77; b) J. Solla-Gullón, A. Rodes, V. Montiel, A. Aldaz, J. Clavilier, *J. Electroanal. Chem.* **2003**, *554*, 273 – 284.
[16] J. Clavilier, J. M. Feliu, A. Fernandez-Vega, A. Aldaz, *J. Electroanal. Chem.* **1989**, *269*, 175 – 189.
[17] V. Grozovski, V. Climent, E. Herrero, J. M. Feliu, *ChemPhysChem* **2009**, *10*, 1922 – 1926.
[18] J. Clavilier, R. Parsons, R. Durand, C. Lamy, J. M. Leger, *J. Electroanal. Chem.* **1981**, *124*, 321 – 326.
[19] S. Trasatti, O. A. Petrii, *Pure Appl. Chem.* **1991**, *63*, 711 – 734.
[20] a) B. Álvarez, V. Climent, A. Rodes, J. M. Feliu, *Phys. Chem. Chem. Phys.* **2001**, *3*, 3269 – 3276; b) A. Gil, A. Clotet, J. M. Ricart, F. Illas, B. Álvarez, A. Rodes, J. M. Feliu, *J. Phys. Chem. B* **2001**, *105*, 7263 – 7271; c) B. Álvarez, A. Berna, A. Rodes, J. M. Feliu, *Surf. Sci.* **2004**, *573*, 32 – 46; d) F. J. Vidal-Iglesias, J. Solla-Gullón, E. Herrero, A. Aldaz, J. M. Feliu, *J. Appl. Electrochem.* **2006**, *36*, 1207 – 1214.

